Topological resilience in non-normal networked systems

Asllani, Malbor; Carletti, Timoteo

Published in:
Phys. Rev. E

DOI:
10.1103/PhysRevE.97.042302

Publication date:
2018

Document Version
Publisher's PDF, also known as Version of record

Topological resilience in non-normal networked systems

Malbor Asllani* and Timoteo Carletti
Department of Mathematics and naXys, Namur Institute for Complex Systems, University of Namur, rempart de la Vierge 8, B 5000 Namur, Belgium

(Received 11 October 2017; revised manuscript received 19 January 2018; published 4 April 2018)

The network of interactions in complex systems strongly influences their resilience and the system capability to resist external perturbations or structural damages and to promptly recover thereafter. The phenomenon manifests itself in different domains, e.g., parasitic species invasion in ecosystems or cascade failures in human-made networks. Understanding the topological features of the networks that affect the resilience phenomenon remains a challenging goal for the design of robust complex systems. We hereby introduce the concept of non-normal networks, namely networks whose adjacency matrices are non-normal, propose a generating model, and show that such a feature can drastically change the global dynamics through an amplification of the system response to exogenous disturbances and eventually impact the system resilience. This early stage transient period can induce the formation of inhomogeneous patterns, even in systems involving a single diffusing agent, providing thus a new kind of dynamical instability complementary to the Turing one. We provide, first, an illustrative application of this result to ecology by proposing a mechanism to mute the Allee effect and, second, we propose a model of virus spreading in a population of commuters moving using a non-normal transport network, the London Tube.

DOI: 10.1103/PhysRevE.97.042302

I. INTRODUCTION

Ecological resilience [1] is the ability of ecosystems to respond to challenges such as fires, windstorms, deforestation, flooding, or the presence of invasive species and their aptitude to return close to the initial state. The way rapid climate changes are affecting the natural habitats [2] and how increasing human activity has been responsible for environmental disasters [3] are the focus of recent studies. On the other hand, resilience is encountered also in human-made systems such as power grids or communications systems where a failure of a component of a system of interconnected elements can trigger a cascade of failures of successive components [4]. In this case, the response of the system is directly correlated to the structural changes in the networked support where the dynamics occurs [5]. Efforts have been made to understand how complex interactions influence the system's resilience [6] in order to optimize the design that enhances their robustness and reduce their vulnerability [7].

Here we show that the resilience of dynamical systems evolving on a complex network is highly determined by the degree of non-normality characterizing the underlying network. This technical definition [8], based on the nonexistence of a suitable orthogonal basis of eigenvectors [9], will be proved in the following to determine an unexpected system response to small disturbances. We anticipate that this abnormal behavior follows a transient amplification process during the initial linear regime which, if sufficiently large, leads subsequently the system to another state, the latter being possibly characterized by spatial inhomogeneities and potentially far from the initial one, reducing thus the system resilience. The non-normality has been previously considered in different domains, e.g., hydrodynamic stability [10], non-Hermitian quantum-mechanics [11], synchronization of networked optoelectronic devices [12], ecology [13], population dynamics with the emphasis to the emergence of deterministic spatial patterns [14,15], or taking into account the stochastic dynamics [16].

To introduce our work, we first illustrate the concept of non-normality borrowing the idea from the community matrix presented in Ref. [13] in the framework of ecology and then we generalize it to dynamical systems defined on complex (non-normal) networks. Let us stress that the framework we propose is different from the latter ones mentioned above. Indeed, the effect of the non-normality, which enters through the network structure, allows us to potentially consider applications to complex systems where the geometry of the spatial interactions play a crucial role. In contrast with the results we mentioned above, the non-normality condition in networked systems is easier to be satisfied because it depends solely on their structure, bypassing any dependence on the dynamical system defined on it. The goal of this paper is thus to bring to the fore a general structure to accommodate for a better understanding of the impact of the non-normality assumption on the resilience of networked systems. To this aim, we here introduce the concept of *non-normal network*, a general paradigm which formalizes the non-normal dynamics in the context of networked complex systems, and, anticipating our following discussion, we state that a network is non-normal if its adjacency matrix does.

As previously stated, the transient amplification due to the network non-normality can push the system into a new state, possibly far from the initial one, and usually exhibits spatial inhomogeneities (patterns). For this reason we show in the second part of the paper that the proposed mechanism could be an alternative pathway to the emergence of spatially

*malbor.asllani@unamur.be

self-organized heterogeneous patterns. One of the mostly diffused mechanism responsible for the patterns formation is the one introduced by Turing, for which a minimal system of two species, activator and inhibitor, can generate complex patterns following a diffusion-induced instability, the celebrated Turing patterns [17,18].

A link between Turing patterns and non-normal operators has been previously proposed in the literature [14–16], in particular in the first reference authors proved that non-normality of the Jacobian matrix is a necessary condition to have Turing patterns for systems involving at least two diffusing species in a continuous domain. We differentiate from the latter because the main "source" of non-normality is in our case the non-normal network on which the dynamics occur. A relevant consequence of this hypothesis is that we can assume symmetric reaction terms, i.e., the Jacobian of the reaction part is a normal matrix, and still obtain patterns. In particular, we are able to prove that a single inhibitor species allowed to freely diffuse on a non-normal network can experience a patchy solution because of the transient instability induced by the non-normal topology; observe that such an outcome is impossible in the framework proposed in Refs. [14–16]: A single species yields, by definition, a normal matrix and so the only way for the non-normality to emerge relies on the diffusion matrix, which instead turns out to be symmetric in the case of continuous support. In conclusion, the present result is complementary to the Turing one and further generalizes the paradigm of patterns formation to broader scenarios that the ones found in the literature.

For a sake of concreteness, we present two relevant applications of the above proposed framework. The first major example here developed that illustrates the importance of this interesting mechanism is the deviance from the Allee effect [19], the principle according to which initial low densities of a given species may critically endanger its survivability as first observed by W. C. Allee. Indeed, Allee remarked that goldfishes grow more rapidly when there are more individuals in a given reservoir [20], an observation that allowed him to draw the conclusion that segregation and cooperation can improve the survival rate. We show that the transient growth, induced by the non-normal network of interactions, may unexpectedly reverse this property, leading to the survival of the population. This could thus provide an effective solution to the problem of reinsertion of new animals into an ecosystem.

There are, however, circumstances where the Allee effect has a positive impact on the population under scrutiny and we want to amplify it. This is the case of virus spreading, where the goal is to reduce the chances for the pathogen to spread by action of the substrate on which the dynamics evolve. Based on this idea, we proposed a simplified model of measles spreading in a population of human beings, commuting using the London Tube network, that can improve our understanding of epidemics spreading in an urban environment [21,22].

The paper is organized as follows. We first set the general behavior of dynamical systems evolving on non-normal networks and we present the main outcomes using a simple model. We then introduce a model to generate networks with a controlled degree of non-normality. Hence, we present three main applications of the proposed framework: a model to mute the Allee effect, a new paradigm for patterns formation of networked systems, and a model of epidemic spreading. We finally discuss our results and draw the conclusions.

II. NON-NORMAL DYNAMICS IN NETWORKED SYSTEMS

Complex interactions in systems, usually constituted by a large number of components, can often be encapsulated in a graph representation through the adjacency matrix $\mathbf{A}$ whose entries $A_{ij} = 1$ if the node j is directly connected to node i and zero otherwise [23]. If also the node i is directly connected to node j determines whether the network is directed or not, a condition that can have a strong impact on the system dynamics.

Let us consider the following generic dynamical system made of M nonlinearly coupled components:

$$\frac{dx_i}{dt} = f(x_i) + \sum_{j=1}^{M} A_{ij} g(x_i, x_j), \tag{1}$$

where $\mathbf{x} = (x_1, x_2, \ldots, x_M)$ is the vector of the system states and $f(\cdot)$, respectively, $g(\cdot,\cdot)$, is a nonlinear function defining the local dynamics occurring on each node i, respectively, the interaction dynamics triggered by the network topology encoded into the adjacency matrix $\mathbf{A}$. Obviously, the evolution of the states of the system will directly depend on the structure of network. Despite the nonlinear nature of the system, one can often obtain a good description by linearizing close to an equilibrium solution of Eq. (1). For the sake of completeness, let us assume a diffusive-like linear coupling, namely g depends linearly on $x_i - x_j$, and consider thus a linear model of a diffusion process on a network with a damping factor, represented by sinks located at each node, namely $\dot{\mathbf{x}} = -a\mathbf{x} + D\mathbf{L}\mathbf{x}$, where a is the decaying rate (assumed for simplicity to be the same for all nodes) and $\mathbf{L}$ the discrete Laplacian matrix, $\mathbf{L} = \mathbf{A} - \mathbf{k}^{\text{out}}$, where $\mathbf{k}^{\text{out}}$ is the diagonal matrix of the connectivities, namely the number of outgoing edges from each node. If the matrix $\mathbf{A}$ is non-Hermitian, then a basis formed by linearly independent eigenvectors or a unitary basis may not exist, and observe that the same holds true for $\mathbf{L}$ by its very first definition. We are hence dealing with a non-normal matrix [8] and the spectrum of the eigenvalues fails to capture the linear dynamics behavior occurring on such non-normal network which deviates from the trivial exponential decay.

A simple but prototypical example, containing all the relevant features, for studying the resilience response of the networked system in non-normality conditions is shown in Fig. 1, where we represent two networks built on a unidirectional ring. The first network has a full rotational symmetry, each vertex has one incoming link and an outgoing one. When the system is perturbed around its unique and stable state $\mathbf{x}^* = (0, \ldots, 0)$, independently of the initial conditions or of the size of the network, the system converges asymptotically to zero [see Fig. 1(a)]. However, if a failure in the system occurs, e.g., a single link is removed (as in the second network), and if the diffusion is stronger than the decay rate, $D/a \gg 1$, then we observe that the unique node with just a single incoming link will exhibit a transient growth before it turns again toward

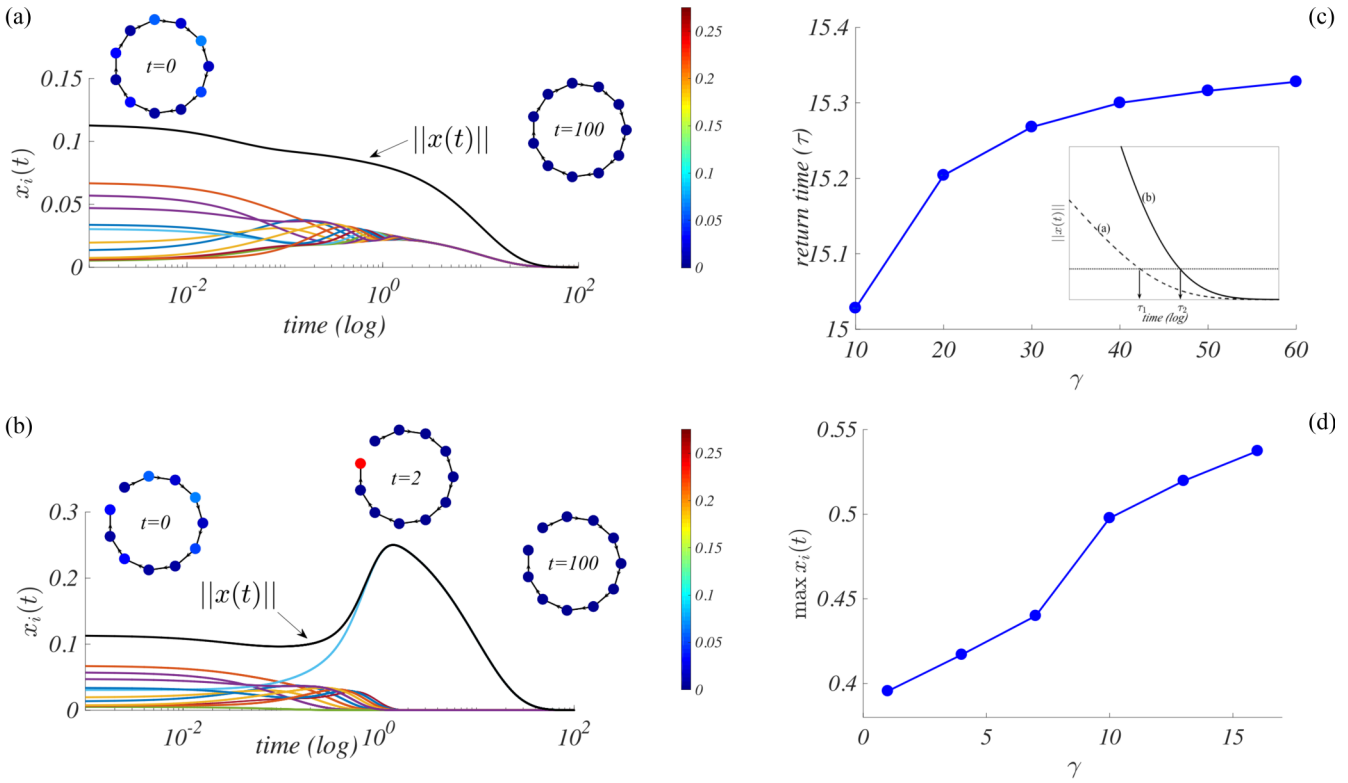

FIG. 1. Transient growth and non-normality in a linear generic example. We represent the time evolution of the node density $x_i(t)$ [colored curves in panels (a) and (b)] for the linear model, $\dot{\mathbf{x}} = -a\mathbf{x} + D\mathbf{L}\mathbf{x}$, on top of a unidirectional (a) ring and (b) path, both made of $M = 11$ nodes. The norm $||x(t)||$ (black curves) describes the global behavior of the system. The model in panel (a) corresponds to a *normal* system and thus, independently of the system parameters and the initial conditions close to the equilibrium point, the perturbations are doomed to die out. On the other hand, using a *non-normal* network (b), and assuming diffusion to be faster than the capture rate into the nodes sinks ($D \gg a$), then the density on the terminal node experiences a strong transient amplification before reaching definitively the equilibrium. This transient regime will influence also the *return time* [see panel (c)] where the return time τ_2 corresponding to the non-normal network in (b) is larger than the return time τ_1 associated to the network used in (a). Observe that the stronger the system non-normality, the longer the return time and also the larger gets the transient deviation from the stable equilibrium as measured by $\max x_i(t)$ [panel (d)]. For both networked systems we used the same initial conditions and the parameters $a = 0.1$ and $D = 10$.

the zero state [see Fig. 1(b)]. We can intuitively explain such behavior by observing that if the individuals diffuse much faster than they are removed from the system due to the sinks, then they will first accumulate in the terminal node from where they cannot exit anymore and thereafter, on a longer timescale, they will inexorably decay. This transient regime will eventually effect the *return time*, the time the system needs to return sufficiently close to the initial state. In Fig. 1(c), we show that the return time is longer for the non-normal system (dark solid curve in the inset) than for the normal one (dashed curve in the inset). We define such behavior the *topological resilience* of a non-normal network. Observe also that, as one should expect, the return time and the maximum deviation from the equilibrium increase as long as the non-normality gets stronger [see Figs. 1(c) and 1(d)], as measured by the parameter γ (see Sec. III).

Let us observe that the above-described phenomenon, i.e., a link failure and the associated increase of non-normality, can trigger a series of similar phenomena where the successive terminal nodes (and links) stop to properly work because of the large transient induced by the non-normality, creating thus a cascade of events [4,6]. Such a possibility is not restricted to ringlike structures but it applies to general non-normal network that we will present in the following section.

III. NON-NORMAL NETWORKS

The key point is now to translate the information of matrix non-normality onto the networks. Said differently, which are the networks that can manifest non-normal dynamics? A complete and exhaustive answer has not yet been provided, although particular cases that involve the non-normality of linear operators have already been identified [11,24–26]. Anticipating our result, we can say that sparse random networks whose nodes are accommodated into directed chainlike structures—in our case responsible for a directional flow into the network—have a good degree of non-normality. Such structures translate into triangular adjacency matrices $\mathbf{A}$ or with similar asymmetric properties. Let us observe that the prototypical network model introduced in Fig. 1 can be used as backbone for the required non-normal network; starting from this remark, we thus propose an algorithm to create a directed and weighted small-world network [27] based on the Newman-Watts mechanism [28] that will result

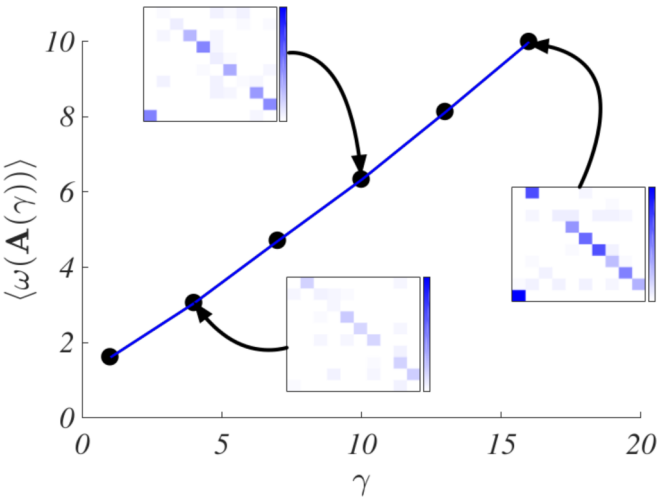

FIG. 2. Numerical abscissa as a function of the directional parameter γ in a non-normal network. Each point has been obtained with 100 replicas using the same set of parameters. For $\gamma = 4, \gamma = 10$, and $\gamma = 16$ we show three representative adjacency matrices; the darker the blue the larger the value of the link weight. One can appreciate the presence of a ringlike structure: The weights on the upper diagonal are quite strong as well as the weight connecting the node N to node 1 (bottom left corner in the matrices).

non-normal. More precisely, we initially take a random weighted directed 1D ring, whose weights are chosen from the uniform distribution $U[0,\gamma]$ with $\gamma > 1$; assume to order nodes in the ring such that the existing links connect node ith with node $(i+1)$th. Observe that the ring is closed; however, due to the different weights, some weak link could act as an effective break, enhancing thus the non-normality. This core directional network mimics the fact that agents are all forced to move in the same direction; γ represents thus a sort of directionality parameter in the backbone network. However, for the sake of generality, one may consider agents to still have some inertia to move in the opposite direction, even if with a very low probability. To reproduce this fact, we assume that weak links, whose weights are of order 1, and thus smaller than the weights in the initial ring of order γ, may also exist pointing in the opposite direction. More precisely, for all $i = 1, \ldots, N$ with probability $0 < p_1 < 1$ we create a weak link from node $(i+1)$-th pointing to node ith. Finally, in complete analogy with the small-world model, long-range links do exist with weights still of order 1: Direct interaction between far away nodes is allowed but it is less probable and weaker with respect to closer ones. More precisely for all couples of node (i,j) such that $|i-j| \geqslant 2$, we add with probability $0 < p_2 < 1$ a directed link whose weight is of order 1.

In Fig. 2 we show three different examples of non-normal networks made by $M = 10$ nodes with $p_1 = 0.5$ and $p_2 = 0.2$ for three different values of the parameter $\gamma = 4$ (weakly non-normal), $\gamma = 10$ (non-normal), and $\gamma = 16$ (strongly non-normal). As one can appreciate as γ increases, the numerical abscissa $\omega[\mathbf{A}(\gamma)]$ [see Eq. (A1) in Appendix A] also gets, on average, larger. We decided to let γ vary because its impact is stronger than the one of p_1 and p_2; indeed, as p_1 increases the Jordan blocks tend to have smaller size while increasing p_2 makes the matrix denser.

The resulting adjacency matrix, although not being exactly a Jordan block, will result strongly non-normal, because of the large values of γ and of the wide distribution of the weights on the main ring with respect to the remaining ones. The algorithm can also be easily extended to a structure where multiple Jordan blocks are present or by defining the weights of the long-range links to be inversely proportional to the geodesic distance. Note that the adjacency matrices generated so far by the algorithm are non-normal but not stable in general. In order to observe the transient growth in the short-time dynamics, it is necessary to assume also the matrix to be stable. This latter fact is surely achieved once one considers the whole dynamical system, namely taking into account also the reaction part and the Laplacian matrix.

IV. MUTING OF THE ALLEE EFFECT

The non-normal assumption is thus responsible for unexpected outcomes on the dynamics and the transient phase can negatively impact the system resilience, and as already stated this feature is related to a structural property of the network. To illustrate the potentiality of this mechanism we describe a major application in ecology, the Allee effect [19] used to explain the community cooperation or facilitation phenomena. A notable example of the latter is the African wild dog, *Lycaon pictus*, endemic and widely spread out over a large geographical area of Africa [29]. Yet rapid climate changes leading to the desertification and fragmentation of the habitat from the agriculture expansion are increasing their risk of extinction. Cooperation among the hunting strategy, the raising of cubs, and defense from bigger predators play a crucial role in the survivability of the species [29]. In the literature, the Allee effect is often introduced by modifying some generic model of population growth, for instance, the logistic equation [18] [see Fig. 3(a)]. It is clear that species will survive only if the initial density is beyond a certain threshold A; the system indeed possesses two (stable) states: an undesired one which corresponds to extinction, $x_1^* = 0$, and the desired one, $x_2^* = 1$, where the system maximizes its opportunities to survive taking into account the available resources [30].

To go one step further in the modeling, let us assume the population of a single species to live in a patchy environment where animals can move across the niches; the dynamics can thus be described by the following diffusively coupled equations:

$$\frac{dx_i}{dt} = r x_i(1-x_i)\left(\frac{x_i}{A} - 1\right) + D\sum_{j=1}^{M} L_{ij}x_j, \forall i\,, \qquad (2)$$

where x_i denotes the species density in the ith patch, r the reproduction rate, A the Allee coefficient, and D the diffusion coefficient, all assumed for simplicity to be the same for all patches.

If species x diffuses using a network that satisfies a normality condition and the initial conditions do not exceed the Allee threshold, $x_i(0) < A\,\forall i$, then the species goes extinct and diffusion cannot prevent it. Conversely, if the underlying network belongs to the family presented above (see Sec. III

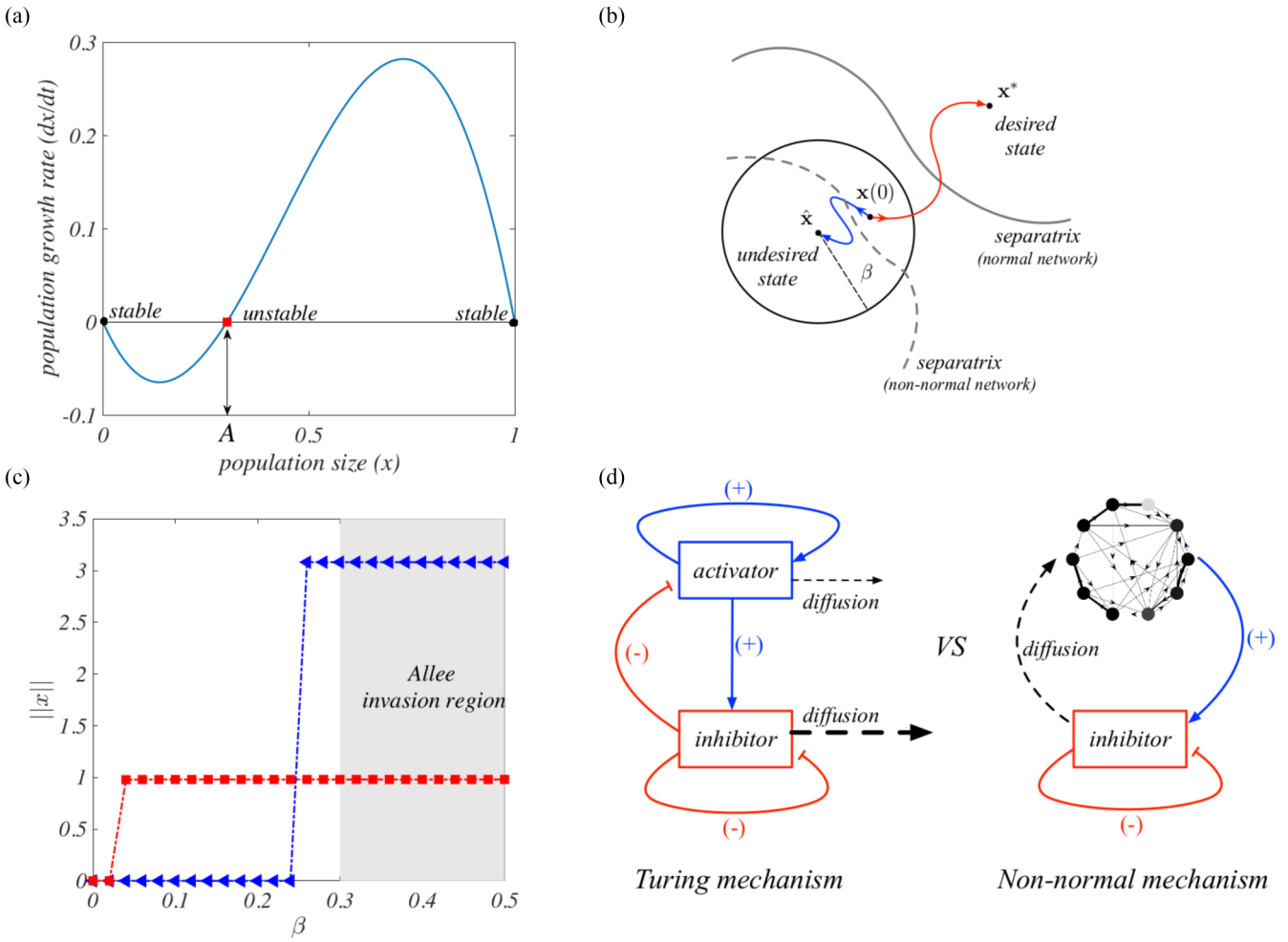

FIG. 3. Resilience and the Allee effect. (a) The nonspatial Allee model, $dx/dt = rx(1-x)(x/A-1)$, in normalized variables, $x = n/K$, where n is the population size and K the carrying capacity, r intrinsic growth rate, and A Allee critical parameter (here $A = 0.3$). The Allee effect states that for $x(0) < A$ the species fails to survive. (b) Non-normal versus normal system. For the normal systems, an initial condition $\mathbf{x}(0)$ converges to the stable state $\hat{\mathbf{x}}$ of the attraction basin it belongs to, while if the numerical abscissa is large enough, hence the transient phase is strong enough, it can reach another stable solution $\mathbf{x}^*$. (c) Bifurcation diagram of the networked Allee model. For a normal system (blue), the size of the survival zone, $\sim 1-0.25 = 0.75$, is very close to that of the nonspatial model, $1 - A = 0.7$, on the other hand for non-normal systems (red) the survival zone is strongly increased, $\sim 1-0.05 = 0.95$. (d) Turing patterns mechanism versus the non-normal one. In the former two species are needed, with the inhibitor diffusing faster than the activator (denoted by a thick dashed line); in the non-normal scheme only one inhibitor species is enough to create patterns once it diffuses on a non-normal network playing the role of the activator.

and Fig. 2), the system fate turns upside down and the population will survive, reducing thus the system resilience. The explanation for this behavior can be found in the competition between the diffusion mechanism and the reproduction rate. It can happen that the transient amplification induced by the non-normality is strong enough to surpass the Allee threshold, at least in some of the patches, and, consequently, the system saturates avoiding the extinction. A schematic illustration of the resilience response of the Allee model on a non-normal network is presented in Fig. 3. The non-normal spatial support makes the stable undesired equilibrium $x_1^* = 0$ less robust against perturbations and thus a larger set of initial conditions close to the latter can in fact escape and end up in a new survival state $\mathbf{x}^*$, close to the second stable equilibrium $x_2^* = 1$ [see Figs. 3(b) and 3(c)]. Let us observe that the non-normality assumption shrinks the attraction basin of $x_1^* = 0$ and the separatrix among the attraction basins shifts towards $x_1^* = 0$.

In conclusion, the effect of the non-normality is to reduce the system resilience and it emphasizes the great advantage that a suitable network topology can represent in the population dynamics. The theoretical approach hereby discussed is generic and can be used to describe different scenarios in ecology, e.g., the introduction of new individuals in a particular habitat with the goal of species conservation or biological control from invasive species [29]. Often, the achievement of such goals is strongly conditioned by the Allee effect, the new introduced individuals are not quite numerous and to prevent their extinction, repeated releases are necessary before the establishment of the new introduced species. However, if the dispersion locations in the ecosystem under study are chosen to induce a non-normal behavior, as previously shown, then this

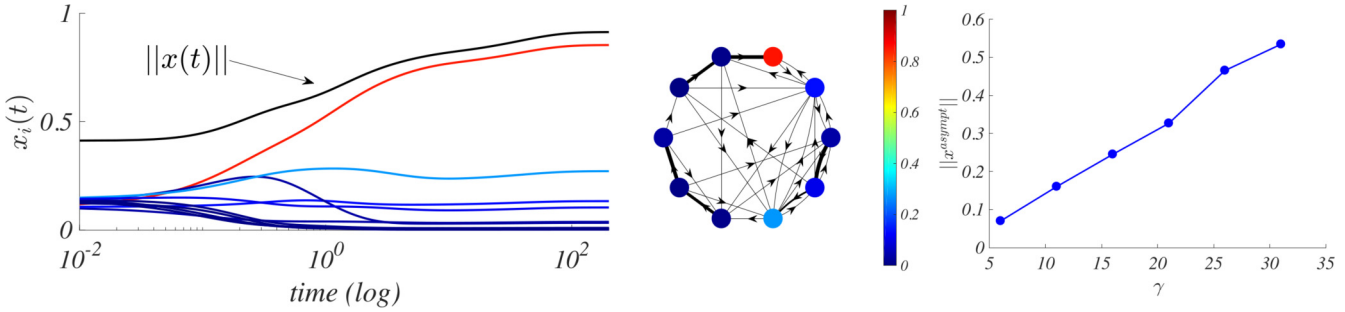

FIG. 4. Patterns emergence in non-normal networked systems. We represent the time evolution of the node density $x_i(t)$ (colored curves on the left panel) for the Allee model (2) on top of a non-normal network made of $M = 10$ nodes(middle panel), together with the norm $||x(t)||$ (black curve) to appreciate the global behavior of the system. One can observe the onset of a stable spatial patterns instigated by a "terminal node" (red node on the middle panel and red curve on the left panel) of a backbone directed weighted path. On the right panel the patterns amplitude measured by $||x(t)||$ for large enough t is reported as a function of γ (black curve), a proxy for the non-normality strength (see Appendix A). Parameters are $r = 0.1$, $A = 0.3$, and $D = 10$. The core ring has stronger links compared to the long-range ones.

will increase the probability of the newly introduced species to survive.

V. A NEW MECHANISM FOR PATTERNS FORMATION

The outcome of the above-presented example, i.e., species survival and nonhomogeneous spatial distribution because of the non-normality assumption, can thus be considered as a mechanism for the formation of nonhomogeneous patterns. One of the mostly diffused mechanisms responsible for the patterns formation is the one introduced by A. Turing in his seminal paper on morphogenesis [17]. He stated that a nonlinear reaction-diffusion system, starting from a homogeneous stable state, can experience a diffusion-driven instability, producing spatially inhomogeneous solutions, the celebrated Turing patterns [17,18]. The minimal required conditions are the presence of at least two species, one being the "activator" (capable to trigger their own growth) and the other the "inhibitor" (antagonist to the former, impede any further growth once diffusing), and, moreover, that the ratio of their diffusion coefficients (inhibitor vs. activator) should be larger than some threshold, which in realistic models is of the order of $\sim$10 [18] (see Fig. 4).

Even though the advantage of the directed network over undirected ones has been emphasized in the process of the formation of Turing patterns [31], the non-normality of the discrete spatial support has not yet been considered. In the presented scenario, this topological feature will force the inhibitors in some of the nodes to initially increase their concentration until they saturate in the nonlinear phase. What is remarkable is that the species which apparently tends to go extinct because of the negative growth rate exploits a faster diffusion process that makes them spread before the individuals counteract and eventually lead to self-organization. This is thus a new mechanism, different from the Turing one, capable of explaining the patterns formation process.

Let us stress again that the present result is a natural generalization of the non-normal community matrices presented in Ref. [13] from the field of the ecology to generic dynamical systems defined on complex networks. Using Weyl's theorem, in Ref. [14] authors have been able to prove that non-normality of the Jacobian matrix of the whole system, evaluated at the equilibrium, is a necessary condition to have Turing patterns for systems involving at least two diffusing species in a continuous domain. Our result differs from the latter because the non-normality can be introduced into the system through a non-normal network; this allows us to relax the assumption on the reaction part that can now be symmetric, i.e., the Jacobian of the reaction part is a normal matrix, and still the system exhibits patterns at odds with the results proposed by Refs. [14–16]. Eventually, this allows us to consider a single (self-inhibiting) species diffusing on a non-normal network—that will act as an activator—as a minimal model for patterns formation. This could introduce a possible explanation of the challenging problem concerning the initial phase of embryogenesis when all the cells are identical and a networked spatial organization of the cells occurs [32,33].

VI. ALLEE EFFECT AND THE OUTBREAK OF EPIDEMICS: A TOY MODEL BASED ON THE LONDON TUBE

Ecosystems are fragile systems and thus ideal study cases for the resilience phenomenon. We have previously seen that there are examples of species dynamics where, in case of low densities, the growth rate is negatively correlated with the population density, meaning that there is the need for a minimum number of individuals to reproduce and survive in their habitat, e.g., the Allee effect. The reasons for the Allee effect are found in the loss of genetic diversity of the population for low densities [29], the demographic stochasticity including the sex-ratio fluctuations which impede reproduction [34] or the reduction of the cooperative interactions when there are few individuals [20]. The latter is of course directly related to the network of interactions and as we have seen to the non-normal dynamics.

On the other hand, the Allee effect may yield also a positive effect when it manifests in the persistence of pathogens as is the case of the measles [35]. It has been observed that the critical community size for measles, namely the minimal number of humans needed for the disease to spread overall in a population of susceptible individuals, is between 250 000 to 400 000. This largely explains why vaccination programs in developing countries, involving only a fraction of the total population, have

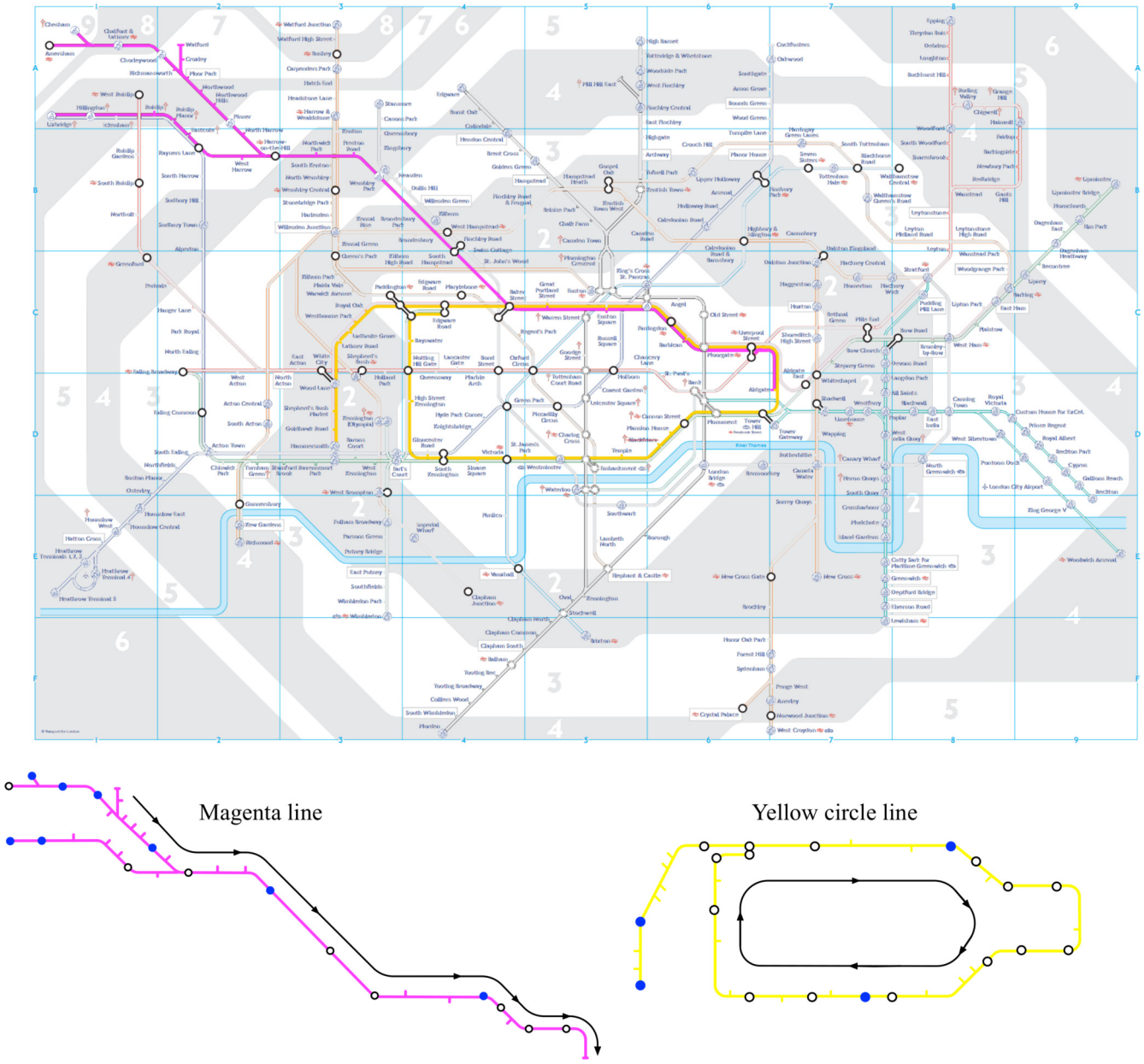

FIG. 5. The London Tube map. Top panel: The whole London Tube map where the yellow Circle Line and the magenta Metropolitan Line have been emphasized to show their different geographical emplacement and shape. In the bottom panels we separately present the magenta line (left) and the yellow line (right) and their respective flows of commuters (black lines with arrows).

nevertheless produced an appreciable decrease in the number of infected individuals.

We hereby thus consider a second relevant application of non-normality in the framework of epidemics spreading on metropolitan scales. We analyze an abstract spreading model based on the London Tube network and we emphasize the role of commuters during the peak hours coming from the outskirts of Greater London, in the outbreak of the epidemics of some pathogens that manifest a strong Allee effect, such as the measles virus.

We consider two principal lines of the London Tube (Fig. 5) that share different topologies and transport features. The first one is the yellow Circle Line (bottom right panel, Fig. 5) which encircles the city downtown and has intersections with almost all the other lines. It is geographically dense, namely the stations are very close each other, and it is one of the lines of the London underground system with the largest number of transported passengers [36], making it a perfect example to test epidemics spreading. The hypothetical pathogen we are considering, say, the measles, is strongly affected by the Allee effect, so in order for the epidemics to outbreak, we need a critical number of vectors, namely infected humans, in the same place for a given amount of time. In Fig. 6(a), we show the result of the simulation of the spatial Allee model once the underlying network is represented by the yellow Circle Line; because only people traveling in the same train can get infected (the pathogen is transmitted by air), we consider only one direction of the line and thus assume the network to be

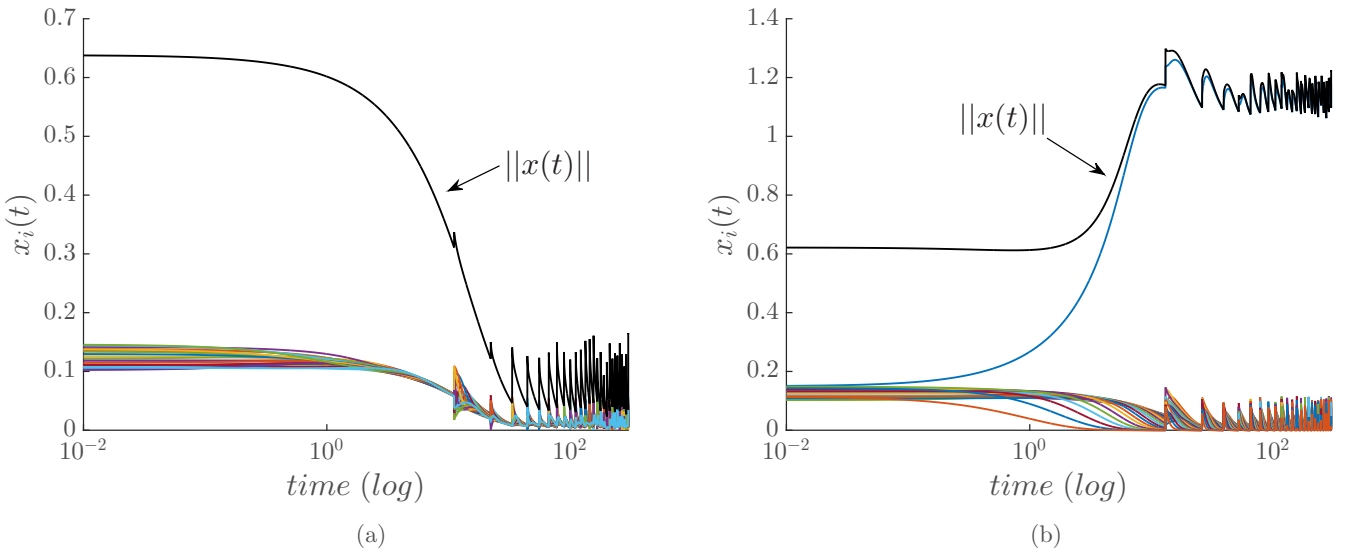

FIG. 6. Hypothetical measles outbreak in the London Tube network. Time evolution of the (normalized) number of infected individuals during the peak hours in the yellow Circle Line taking into account 27 stations (a) and in the magenta Metropolitan Line (b) considering 23 stations with the fluxes illustrated in Fig. 5. In the former case (a) we assumed the average number of passengers to be constant because in each station, the average number of passengers getting on equals that of those getting off. The circular topology and the Allee effect impede the outbreak of the epidemic. On the contrary, for the second case (b), we assume that, on average, as long the trains approach downtown, the number of passengers increases, because most of the individuals have their destination in the city center. In this case, despite the presence of the Allee effect, the topology contributes to the outbreak of the measles epidemic once the train reaches the center. The parameters of the Allee model are $a = 1$, $A = 0.3$, and $D = 10$ for both cases.

directed. Moreover, we assume that, on average, the number of people in the train to remain constant for the time interval we consider. Namely because of the density of the stations and of the centrality of the line, roughly the same number of people gets in and off the train at each station. The random variations from the average is responsible for the fluctuations visible in the Fig. 6. The main outcome one can appreciate from Fig. 6(a) is that the disease does not persist and the epidemics will not outbreak, at odds with the intuition that the Circle Line will support many commuters and thus inducing a high chance for the virus to survive due to the large number of human encounters.

On the other hand, if we consider the magenta Metropolitan Line (bottom left panel of Fig. 5), which connects the north-western outskirts with the downtown of London, and perform a similar hypothetical experiment of virus spreading, the result overturns [see Fig. 6(b)]. Here we assume that passengers for the period of time we considered mostly do not get off the train until they reach the center of the city. This induces a strong directionality in the network, which will result non-normal, thus allowing the virus to overcome the Allee threshold. It is now clear from the simulation that the epidemic outbreaks; once the commuters reach their destinations at the center of the city they are almost all infected and then they will contribute to spreading the virus in the central part of the city and then, as a consequence, in the whole city.

This phenomenon can be easily explained in the framework of non-normal dynamics. The Circle Line can be seen as a normal network and, moreover, commuters spend, on average, a short time on these trains, independently from the fact that they are vectors of the virus or not; in conclusion, the pathogen does not have sufficient time to develop and reach numbers that allow it to invade the population where it diffuses. On the contrary, possible vectors (commuters) living in the suburbs of the city and spending a longer time in the densely populated train make possible the spread of the virus, because of the non-normality structure of the network, as in the case of the Metropolitan Line.

In conclusion, with this simple model we have been able to show that independently from the topology of the spatial domain, if—by their actions—the individuals determine a strongly directed flux from one region to another, then the spreading pathogen will avoid the Allee effect and so helping its survivability. This observation could play a relevant role in the modeling of diseases spreading in urban scenarios.

VII. DISCUSSION

In this paper we studied the role of non-normal topology on the resilience phenomenon for dynamical systems defined on directed networks. In the first part, we showed that, interestingly enough, the way that parts of interconnected systems interact could make them vulnerable to weak external perturbations. Unexpectedly, these perturbations will follow an initial amplification that can lead the system to a new state, possibly far from the initial one. Hence to increase the robustness of the networked system, for instance, in the case of power grids aimed at reducing cascade failures, one should tune down the non-normality.

Furthermore, we proved in the second part of the paper that once the non-normality guides the system toward a nonhomogeneous equilibrium state, the process at work can be

cast in the framework of patterns formation driven by dynamical instability. The single species case hereby presented shows the impact of the network topology on the self-organization process, allowing the formation of patterns complementary to the Turing mechanism, thus resulting in the minimal model for pattern onset on networked systems.

From the applicative point of view, this approach may shed light onto problems related to multispecies models in ecology; for instance, if the goal is to promote coexistence or survival of newly introduced species, then the network of interactions should be designed to be non-normal as much as possible to prevent the Allee effect from favoring extinction. On the other hand, in the case where the invasive species is an infectious pathogen [37] (noxious Allee effect), then one should avoid or reduce non-normality.

This last remark can thus have a very relevant impact on the design of urban agglomerations and their transportation networks in order to increase their robustness against the spreading of diseases. As a particular study case we mention the London Tube transport system, where the daily commuting fluxes from the outskirts to the city center create a non-normal system where the possibility for pathogens to survive and the consequent epidemic outbreaks are highly enhanced compared to people living and moving in the downtown.

Let us observe that the non-normal mechanism studied is more general than the few applications we brought here, as one can infer from Eq. (1). In particular, we decided to focus on the diffusion process and the role of space; nevertheless, one can provide interesting applications also to a-spatial systems where the non-normality shapes the interactions among individuals of different species, for instance, in the framework of food webs where the non-normality assumption holds very often (see Table I in Appendix C). Indeed, food webs are very often directed acyclic graphs (or very similar to them) that by definition have strongly non-normal adjacency matrices. In conclusion, we are confident that the non-normality property can determine multiple and still unexplored achievements in the dynamics of networked systems.

ACKNOWLEDGMENTS

The work of M.A. and T.C. presents research results of the Belgian Network DYSCO, funded by the Interuniversity Attraction Poles Programme, initiated by the Belgian State, Science Policy Office. The work of M.A. is also supported by a FRS-FNRS Postdoctoral Fellowship. The authors acknowledge D. Fanelli, G. Deffuant, and R. Lambiotte for reading the manuscript.

APPENDIX A: NON-NORMALITY MEASURES AND TRANSIENT GROWTH

Non-normal linear dynamical systems exhibit a peculiar time evolution, the transient phase being potentially very different from the case of normal ones. Different measures exist to quantify the non-normality of a matrix [8,14] and thus to unravel the accompanying behavior [38]; for instance, in population dynamics [13] the *reactivity* is used for evaluating

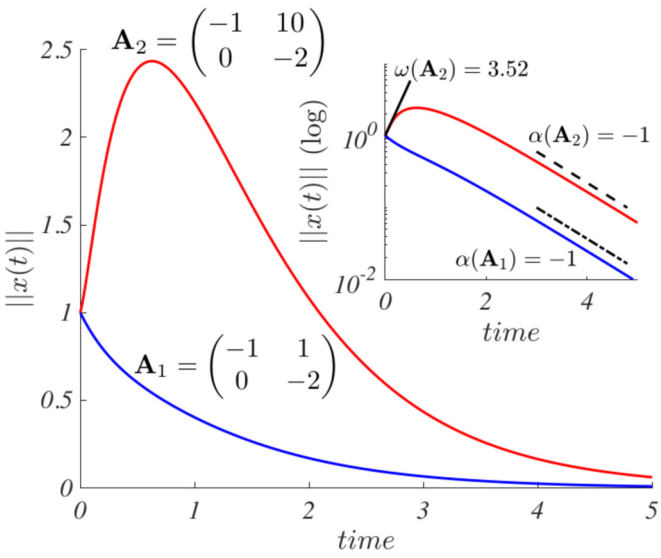

FIG. 7. Time evolution of the norm of the solution of the linear ODE $\dot{\mathbf{x}} = \mathbf{A}\mathbf{x}$. The red curve corresponds to a non-normal matrix $\omega(\mathbf{A}_2) = 3.52$ while the blue curve to a normal one $\omega(\mathbf{A}_1) = -0.79$; one can clearly appreciate the temporal growth arising in the former case. In the inset we still report the norm of the solution but in logarithmic scale to emphasize the short-time behavior described by the numerical abscissa (the straight black line has slope 3.52) and the long-time one related to the spectral abscissa (the dashed and dot-dashed straight lines have slope -1).

the ecological resilience. The latter, referred to as the *numerical abscissa* [8], also suites our purpose. For a given $M \times M$ real matrix $\mathbf{A}$ it is defined by

$$\omega(\mathbf{A}) = \sup \sigma[(\mathbf{A} + \mathbf{A}^*)/2], \tag{A1}$$

where $\sigma(\mathbf{A})$ denotes the spectrum of the matrix $\mathbf{A}$ and $\mathbf{A}^*$ is its conjugate transpose. Let us assume $\mathbf{A}$ to be a stable matrix [39]; if the numerical abscissa takes negative values, then the orbits exponentially approach the fixed point. On the other hand, if $\omega(\mathbf{A}) > 0$, then a transient growth occurs whose size is proportional to the numerical abscissa, determining thus the magnitude of the non-normality of $\mathbf{A}$ (see Fig. 1 and Fig. 7).

In order to study as a single entity the behavior of the linear ordinary differential equation (ODE), $\frac{d\mathbf{x}}{dt} = \mathbf{A}\mathbf{x}$, we can look at the time evolution of the Euclidian norm of the solution $||\mathbf{x}|| = \sqrt{x_1^2 + x_2^2 + \cdots + x_M^2}$. One can easily realize that the latter experiences a temporary growth whose size is proportional to the non-normality of the involved matrix; in the case of multiple eigenvalues (as in the case reported in Fig. 1), we can look at the explicit solution $\mathbf{x}(t) = c_1\mathbf{v}_1 + c_2 t^{M-2} e^{\lambda_2 t}\mathbf{v}_2 + c_3 e^{\lambda_3 t}\mathbf{v}_3$, where c_j are constant coefficients set by the initial conditions; λ_2 and λ_3 the negative eigenvalues of the non-normal matrix, the former with multiplicity $M-2$; and $\mathbf{v}_j$ the associated eigenvectors ($\lambda_1 = 0$). Let us observe that the transient growth for $||\mathbf{x}||$ can be obtained also in the case of nondegenerate eigenvalues once a orthonormal eigenbasis cannot be found (see Fig. 7).

Indeed, the *numerical abscissa* generically describes the short-time behavior of the solution (the limit $t \to 0^+$), in fact calculating:

$$\begin{aligned}
&\max_{||\mathbf{x}_0||\neq 0}\left[\left(\frac{1}{||\mathbf{x}||}\frac{d||\mathbf{x}||}{dt}\right)\Big|_{t=0}\right] \\
&= \max_{||\mathbf{x}_0||\neq 0}\left[\left(\frac{1}{||\mathbf{x}||}\frac{d\sqrt{\mathbf{x}^*\mathbf{x}}}{dt}\right)\Big|_{t=0}\right] \\
&= \max_{||\mathbf{x}_0||\neq 0}\left[\left(\frac{\mathbf{x}^* d\mathbf{x}/dt + (d\mathbf{x}/dt)^*\mathbf{x}}{2||\mathbf{x}||^2}\right)\Big|_{t=0}\right] \\
&= \max_{||\mathbf{x}_0||\neq 0}\left[\left(\frac{\mathbf{x}^*(\mathbf{A}+\mathbf{A}^*)\mathbf{x}}{2||\mathbf{x}||^2}\right)\Big|_{t=0}\right] \\
&= \max_{||\mathbf{x}_0||\neq 0}\left[\frac{\mathbf{x}_0^* H(\mathbf{A})\mathbf{x}_0}{\mathbf{x}_0^*\mathbf{x}_0}\right], \qquad \text{(A2)}
\end{aligned}$$

where $\mathbf{x}_0$ is the initial condition for the solution $\mathbf{x}$. One can recognize that $H(\mathbf{A}) = (\mathbf{A} + \mathbf{A}^*)/2$ is the Hermitian part of $\mathbf{A}$; hence, according to the Rayleigh's principle [39], the rightmost term of Eq. (A2) is equal to the largest eigenvalue of $H(\mathbf{A})$, and thus we can conclude that $\omega(\mathbf{A}) = \sup\sigma[H(\mathbf{A})]$ provides the initial behavior of the norm of $\mathbf{x}$. Notice that this measure does not depend anymore on the initial conditions, meaning that it characterizes the intrinsic properties of the matrix $\mathbf{A}$ and not of a specific solution.

The second limit we are interested in is the long-time behavior of the solution, namely $t \to +\infty$. This can be studied using the *spectral abscissa* of the matrix $\mathbf{A}$, denoted by $\alpha(\mathbf{A})$ and defined by:

$$\alpha(\mathbf{A}) := \max_{||\mathbf{x}_0||\neq 0}\left[\lim_{t\to+\infty}\left(\frac{1}{||\mathbf{x}||}\frac{d||\mathbf{x}||}{dt}\right)\right]. \qquad \text{(A3)}$$

It is well known that the eigenvalue with the largest real part completely determines the asymptotic behavior of the solution of the ODE, and thus one can compute the spectral abscissa as $\alpha(\mathbf{A}) = \sup\Re[\sigma(\mathbf{A})]$.

We can hence conclude by observing that, although $\alpha(\mathbf{A}) < 0$, if $\omega(\mathbf{A}) > 0$, then the equilibrium will be stable but a transient growth will emerge in the short-time regime, producing a deviation from the steady exponential decay of stable normal systems. The following example well illustrates this behavior. Let us analyze the time evolution of the norm of the solution of the linear ODE system involving the following matrices $\mathbf{A}_i$, $i = 1,2$,

$$\mathbf{A}_1 = \begin{pmatrix} -1 & 1 \\ 0 & -2 \end{pmatrix} \quad \text{and} \quad \mathbf{A}_2 = \begin{pmatrix} -1 & 10 \\ 0 & -2 \end{pmatrix}.$$

A straightforward computation allows us to obtain the numerical abscissa, $\omega(\mathbf{A}_1) = -0.79 < 0$ and $\omega(\mathbf{A}_2) = 3.52 > 0$, and the spectral abscissa $\alpha(\mathbf{A}_1) = \alpha(\mathbf{A}_2) = -1$. Although both matrices possess the same spectral abscissa, the existence of a positive numerical abscissa for the second matrix determines a transient growth to occur (see the main panel of Fig. 7). A schematic illustration of the impact of these two measures on the transient time evolution of a solution is given in the inset of Fig. 7. Once again, this prototypical example demonstrates that the spectrum alone is not able to describe the linear dynamics in the setting of non-normal dynamical systems.

APPENDIX B: DETAILS OF THE NUMERICAL SIMULATIONS

Figure 1. The results reported in Fig. 1 have been obtained using a deterministic numerical integration scheme based on a fourth-order Runge-Kutta method. For both Figs. 1(a) and 1(b) the initial conditions were chosen randomly from a uniform distribution [0,0.1]. For both networks, the ring and the path, the links all have weights 1. The return time has been defined as the time needed by the system to return 0.1 close to the initial condition.

Figure 3. To obtain the bifurcation diagram shown in Fig. 3(c) we considered initial conditions close to the ones used for Fig. 1, that is, drawn from a uniform distribution $U[0,0.1]$, and then we numerically simulated the spatial Allee model on top of a non-normal network (red squares) and of a weakly non-normal one (blue triangles), and eventually we determined the asymptotic size of the system described by $||\mathbf{x}||$. The model parameters have been set to $r = 0.1$, $A = 0.3$, and $D = 10$. More precisely, for several values of $\beta \in [0,0.5]$ we draw initial conditions from the uniform distribution $U[0,0.1]$, and then we add a random number drawn from the distribution $U[\beta - 0.05, \beta + 0.05]$; to reduce the variability in the results induced by the randomness of the initial conditions, we repeat 10 times the same experiment with the same β. The non-normal network has been built using the method presented above with parameters $M = 10$ nodes, $\gamma = 10$, $p_1 = 0.5$, and $p_2 = 0.2$, resulting in a numerical abscissa $\omega(\mathbf{J}) = 1.87$. The weakly non-normal network has been obtained similarly but using $p_2 = 0.8$, giving a numerical abscissa $\omega(\mathbf{J}) = 0.57$. Let us observe that we hereby compute the numerical abscissa using the Jacobian of the dynamical system and not only of the network adjacency matrix.

Figure 4. The results reported in this figure have been obtained using a deterministic numerical integration scheme based on a fourth-order Runge-Kutta method. The initial conditions were chosen randomly from a uniform distribution [0,0.1]. $||x^{\text{asympt}}||$ is the value of $||x(t)||$ for t large enough so that the system reached the equilibrium patterns. Let us observe that this is a measure of the pattern's amplitude because the reference solution is the null one. The model parameters have been set to $r = 0.1$, $A = 0.3$, and $D = 10$. The non-normal network has been built using the method presented above with parameters $M = 10$ nodes, $\gamma = 10$, $p_1 = 0.5$, and $p_2 = 0.2$.

APPENDIX C: NON-NORMALITY IN FOOD WEBS

In this section we report some figures of food webs [40], emphasizing in particular their non-normal character (Table I).

TABLE I. Food webs. We report some figures for a large set of food webs available in the literature, whose number of nodes and links span two orders of magnitude. They all result to be (weighted) non-normal networks, namely $\mathbf{A}\mathbf{A}^* \neq \mathbf{A}^*\mathbf{A}$, and they posses a positive numerical abscissa (ω) which is much larger than the corresponding spectral abscissa (α).

Network name	Nodes	Links	$\omega(\mathbf{A})$	$\omega(\mathbf{A}) - \alpha(\mathbf{A})$	Ref.
Charca de Maspalomas, Gran Canaria	21	82	5.40×10^5	2.97×10^4	[41,42]
Crystal River (2)	21	100	1.94×10^3	8.86×10^2	[42,43]
Crystal River (1)	21	125	2.52×10^3	1.31×10^3	[42,43]
Narragansett Bay Model	32	220	8.06×10^5	6.56×10^3	[42,44]
Early Cambrian Chengjiang Shale	33	99	6.33	1.41	[45,46]
Lower Chesapeake (Summer carbon flows)	34	178	1.06×10^5	3.34×10^4	[42,47]
Middle Chesapeake (Summer carbon flows)	34	209	1.65×10^5	3.47×10^4	[42,47]
Upper Chesapeake (Summer carbon flows)	34	215	6.23×10^4	7.76×10^3	[42,47]
Chesapeake (Summer carbon flows)	36	177	4.11×10^5	9.87×10^4	[42,48]
Middle Cambrian Burgess Shale	48	249	7.88	5.88	[45,46]
St Marks River (Florida) Estuary	51	356	139.50	28.45	[42,49]
Everglades Graminoid Marshes	66	916	1.44×10^3	1.04×10^3	[42,50]
Flensburg Fjord (Germany and Denmark)	77	579	10.27	9.27	[46,51,52]
Carpinteria Salt Marsh (USA)	107	970	13.21	7.91	[46,52,53]
Bahia Falsa (Mexico)	119	1077	13.98	9.20	[46,52,53]
Otago Harbor (New Zealand)	123	1206	14.36	8.36	[46,52,54]
Sylt Tidal Basin (Germany and Denmark)	126	1052	13.39	10.78	[46,52,55]
Cypress wetlands South Florida (wet season)	128	2016	296.71	132.11	[56,57]
Cypress wetlands South Florida (dry season)	128	2137	217.60	152.50	[56,57]
Ythan Estuary (Scotland)	134	420	8.13	6.51	[46,52,58]
Estero de Punta Banda (Mexico)	138	1657	18.56	9.56	[46,52,53]
Little Rock Lake (Wisconsin, US)	183	2494	21.69	14.69	[56,59]

[1] L. H. Gunderson, Annu. Rev. Ecol. Evol. Syst. **31**, 425 (2000).
[2] D. Bachelet, R. Neilson, J. M. Lenihan, and R. J. Drapek, Ecosystems **4**, 164 (2001).
[3] W. N. Adger, T. P. Hughes, C. Folke, S. R. Carpenter, and J. Rockström, Science **309**, 1036 (2005).
[4] A. E. Motter and Y.-C. Lai, Phys. Rev. E **66**, 065102 (2002).
[5] J. Gao, B. Barzel, and A.-L. Barabási, Nature **530**, 307 (2016).
[6] S. V. Buldyrev, R. Parshani, G. Paul, H. E. Stanley, and S. Havlin, Nature **464**, 1025 (2010).
[7] J. Asha and D. Newth, Physica A **380**, 673 (2007).
[8] L. N. Trefethen and M. Embree, *Spectra and Pseudospectra: The Behavior of Nonnormal Matrices and Operators* (Princeton University Press, Princeton, NJ, 2005).
[9] In fact, the definition for non-normality for a given matrix **A** is based on the nonexistence of a unitary matrix which diagonalizes it. This means that it is still possible for the eigenvectors of **A** to form a nonunitary base.
[10] L. N. Trefethen, A. E. Trefethen, S. C. Reddy, and T. A. Driscoll, Science **261**, 578 (1993).
[11] N. Hatano and D. R. Nelson, Phys. Rev. Lett. **77**, 570 (1996).
[12] B. Ravoori, A. B. Cohen, J. Sun, A. E. Motter, T. E. Murphy, and R. Roy, Phys. Rev. Lett. **107**, 034102 (2011).
[13] M. G. Neubert and H. Caswell, Ecology **78**, 653 (1997).
[14] M. G. Neubert, H. Caswell, and J. D. Murray, Math. Biosci. **175**, 1 (2002).
[15] L. Ridolfi, C. Camporeale, P. D'Odorico, and F. Laio, Europhys. Lett. **95**, 18003 (2011).
[16] T. Biancalani, F. Jafarpour, and N. Goldenfeld, Phys. Rev. Lett. **118**, 018101 (2017).
[17] A. M. Turing, Phil. Trans. R. Soc. B **237**, 37 (1952).
[18] J. D. Murray, *Mathematical Biology II: Spatial Models and Biomedical Applications* (Springer-Verlag, Berlin, 2001).
[19] W. C. Allee, A. E. Emerson, O. Park, T. Park, and K. P. Schmidt, *Principles of Animal Ecology* (Saunder, Philadelphia and London, 1949).
[20] W. C. Allee and E. Bowen, J. Exp. Zool. **61**, 185 (1932).
[21] R. Pastor-Satorras and A. Vespignani, Phys. Rev. Lett. **86**, 3200 (2001).
[22] V. Colizza, A. Barrat, M. Barthélemy, and A. Vespignani, Proc. Natl. Acad. Sci. USA **103**, 2015 (2006).
[23] M. E. J. Newman, *Networks: An Introduction* (Oxford University Press, Oxford, 2010).
[24] M. Embree and L. N. Trefethen, Proc. Roy. Soc. Lond. A **455**, 2471 (1999).
[25] G. Hennequin, T. P. Vogels, and W. Gerstner, Phys. Rev. E **86**, 011909 (2012).
[26] D. Viswanathan and L. N. Trefethen, SIAM J. Matrix Anal. Appl. **19**, 564 (1998).
[27] D. J. Watts and S. H. Strogatz, Nature **393**, 440 (1998).
[28] M. E. J. Newman and D. J. Watts, Phys. Rev. E **60**, 7332 (1999).
[29] F. Courchamp, T. Clutton-Brock, and B. Grenfell, Trends Ecol. Evol. **14**, 405 (1999).

[30] Let us note that Eq. (2) has been written using the rescaled variable $x_i = n_i/K$, namely the ratio of the number of individuals in the ith patch and the carrying capacity K.
[31] M. Asllani, J. D. Challenger, F. S. Pavone, L. Sacconi, and D. Fanelli, Nat. Commun. **5**, 4517 (2014).
[32] F. Bignone, J. Biol. Phys. **27**, 257 (2001).
[33] R. Schnabel *et al.*, Dev. Biol. **294**, 418 (2006).
[34] R. Lande, Oikos **83**, 353 (1998).
[35] M. J. Keeling and B. T. Grenfell, Science **275**, 65 (1997).
[36] Which is london's busiest tube line? https://www.citymetric.com/transport/which-londons-busiest-tube-line-904.
[37] M. A. Lewis and P. Kareiva, Theor. Popul. Biol. **43**, 141 (1993).
[38] We limit ourselves to the case of continuous-time dynamical systems (ordinary differential equation), the reader must, however, be aware that an analogous theory exists for discrete-time dynamical systems (maps).
[39] G. H. Golub and C. F. van Loan, *Matrix Computations*, 3rd ed. (Johns Hopkins University Press, Baltimore, MD, 1996).
[40] J. Kunegis, in *Proc. Int. Conf. on World Wide Web Companion, Rio de Janeiro, 2013* (ACM 425, New York, 2013), pp. 1343–1350.
[41] J. Almuniaa, G. Basterretxeaa, J. Aristeguia, and R. E. Ulanowicz, Estuar. Coast. Shelf Sci. **49**, 363 (1999).
[42] Pajek datasets, foodwebs, http://vlado.fmf.uni-lj.si/pub/networks/data/bio/foodweb/foodweb.htm.
[43] R. E. Ulanowicz, *Growth and Development: Ecosystems Phenomenology* (Springer-Verlag, NY, 1986).
[44] M. Monaco and R. Ulanowicz, Mar. Ecol. Prog. Ser. **161**, 239 (1997).
[45] J. A. Dunne, R. J. Williams, N. D. Martinez, R. A. Wood, and D. H. Erwin, PLoS Biol. **6**, e102 (2008).
[46] Index of complex networks, https://icon.colorado.edu/.
[47] J. Hagy, Eutrophication, Hypoxia and Trophic Transfer Efficiency in Chesapeake Bay, Ph.D. thesis, University of Maryland, 2002.
[48] D. Baird and R. Ulanowicz, Ecol. Monogr. **59**, 329 (1989).
[49] D. Baird, J. Luczkovich, and R. Christian, Estuar. Coast. Shelf Sci. **47**, 329 (1998).
[50] R. E. Ulanowicz, J. J. Heymans, and M. S. Egnotovich, *Network Analysis of Trophic Dynamics in South Florida Ecosystem*, [umces]cbl 00–0176 ed. (Chesapeake Biological Laboratory, Solomons, 2000).
[51] C. Zander, N. Josten, K. Detloff, R. Poulin, J. McLaughlin, and D. Thieltges, Ecology **92**, 2007 (2011).
[52] J. A. Dunne, K. D. Lafferty, A. P. Dobson, R. F. Hechinger, A. M. Kuris, N. D. Martinez, J. P. McLaughlin, K. N. Mouritsen, R. Poulin, K. Reise, D. B. Stouffer, D. W. Thieltges, R. J. Williams, and C. D. Zander, PLoS Biol. **11**, e1001579 (2013).
[53] R. F. Hechinger, K. D. Lafferty, J. P. McLaughlin, B. L. Fredensborg, T. C. Huspeni, J. Lorda, P. K. Sandhu, J. C. Shaw, M. E. Torchin, K. L. Whitney, and A. M. Kuris, Ecology **92**, 791 (2011).
[54] K. Mouritsen, R. Poulin, J. McLaughlin, and D. Thieltges, Ecology **92**, 2006 (2011).
[55] D. Thieltges, K. Reise, K. Mouritsen, J. McLaughlin, and R. Poulin, Ecology **92**, 2005 (2011).
[56] Trophic networks dataset—KONECT, http://konect.cc/categories/Trophic/.
[57] R. E. Ulanowicz, J. J. Heymans, and M. S. Egnotovich, Annual Report to the United States Geological Service Biological Resources Division Ref. No. [UMCES] CBL 00-0176, Chesapeake Biological Laboratory, University of Maryland (2000).
[58] M. Huxham, S. Beany, and D. Raffaelli, Oikos **76**, 284 (1996).
[59] N. D. Martinez, J. J. Magnuson, T. Kratz, and M. Sierszen, Ecol. Monogr. **61**, 367 (1991).